nature medicine

SUPPLEMENTARY INFORMATION

https://doi.org/10.1038/s41591-018-0025-7

In the format provided by the authors and unedited.

HIV vaccine candidate activation of hypoxia and the inflammasome in CD14$^+$ monocytes is associated with a decreased risk of SIV$_{mac251}$ acquisition

Monica Vaccari[1], Slim Fourati[2], Shari N. Gordon[1], Dallas R. Brown[1], Massimilano Bissa[1], Luca Schifanella[1], Isabela Silva de Castro[1], Melvin N. Doster[1], Veronica Galli[1], Maria Omsland[1], Dai Fujikawa[1], Giacomo Gorini[1], Namal P. M. Liyanage[1], Hung V. Trinh[3,4], Katherine M. McKinnon[5], Kathryn E. Foulds[6], Brandon F. Keele[7], Mario Roederer[6], Richard A. Koup[6], Xiaoying Shen[8], Georgia D. Tomaras[8], Marcus P. Wong[9], Karissa J. Munoz[9], Johannes S. Gach[9], Donald N. Forthal[9], David C. Montefiori[10], David J. Venzon[11], Barbara K. Felber[12], Margherita Rosati[13], George N. Pavlakis[13], Mangala Rao[3], Rafick-Pierre Sekaly[2] and Genoveffa Franchini[1]*

[1]Animal Models and Retroviral Vaccines Section, Vaccine Branch, Center for Cancer Research, National Cancer Institute, Bethesda, MD, USA. [2]Department of Pathology, Case Western Reserve University, Cleveland, OH, USA. [3]US Military HIV Research Program, Henry M. Jackson Foundation for the Advancement of Military Medicine, Bethesda, MD, USA. [4]US Military HIV Research Program, Walter Reed Army Institute of Research, Silver Spring, MD, USA. [5]Vaccine Branch, Center for Cancer Research, National Cancer Institute, Bethesda, MD, USA. [6]Vaccine Research Center, National Institute of Allergy and Infectious Diseases, National Institutes of Health, Bethesda, MD, USA. [7]AIDS and Cancer Virus Program, Leidos Biomedical Research Inc., Frederick National Laboratory, Frederick, MD, USA. [8]Duke Human Vaccine Institute, Duke University, Durham, NC, USA. [9]Division of Infectious Diseases, Department of Medicine, University of California, Irvine School of Medicine, Irvine, CA, USA. [10]Division of Surgical Sciences, Duke University School of Medicine, Durham, NC, USA. [11]Biostatistics and Data Management Section, Center for Cancer Research, National Cancer Institute, Bethesda, MD, USA. [12]Human Retrovirus Pathogenesis Section, Vaccine Branch, Center for Cancer Research, National Cancer Institute, Frederick, MD, USA. [13]Human Retrovirus Section, Vaccine Branch, Center for Cancer Research, National Cancer Institute, Frederick, MD, USA. *e-mail: franchig@mail.nih.gov

Supplementary Figure 1. SIV_{mac251} challenge outcome in vaccinated and control animals. Survival curve of (**a**) 6 concurrent versus 35 historical controls, (**b**) Ad26-SIV versus 6 concurrent + 35 historical controls, (**c**) Ad26-SIV vaccinated animals versus 6 concurrent controls, (**d**) DNA-SIV versus 6 concurrent controls, and (**e**) Ad26-SIV and DNA-SIV vaccinated animals (logrank test). The study was not powered to compare vaccine strategies. (**f**) Number of transmitted variants in Ad26-SIV 9, (**g**) DNA-SIV and (**h**) concurrent controls. Each bar corresponds to each animal. (**i**) SIV RNA levels expressed as geometrical mean ± standard error in plasma and (**j**) percent of $CD4^+$ T cell changes in the blood over time (mean ± standard error) in animals that were infected after 10 x exposures to SIV_{mac251} (12/12 in the Ad26 group, 10/12 in the DNA group).

Supplementary Figure 2. Kinetic of monocytes in blood after different primes. (**a**) Gating strategy to define monocytes subpopulation in blood. CD16 and CD14 are used to defined classical ($CD14^{++}$ $CD16^-$), non-classical ($CD14^{low}$ $CD16^+$), and intermediate ($CD14^{++}$ $CD16^+$) monocytes within HLA-DR^+ cells. Classical monocytes express CCR2 and CXCR4 marker at higher levels than $CD16^+$ monocytes. (**b**) Frequency of monocytes defined as $CD14^+$ $CD16^{+/-}$ HLA-DR^+ in blood of macaques primed with Ad26 or (**c**) DNA before the challenge at 2 weeks from the prime (Ad26 = week 2; DNA = week 6), and at weeks 14 and 27. (**d**) Median ± standard error is shown for the two groups. (**e**) Frequency of blood $CD14^+$ HLA-DR^+ cells, (**f**) non-classical and intermediate cells ($CD16^+$). (**g**) Levels of plasma CCL2 measured after ALVAC-primed (n = 10), Ad26-primed (n = 12) or DNA-primed (n = 12) ALVAC-SIV + gp120 alum vaccine. The Kruskal-Wallis test corrected for multiple comparisons was used.

Supplementary Figure 3. Identification of two monocytic signatures associated with a reduced risk versus an increased risk of SIV acquisition. (**a**) Radial plot showing the relative contribution of immune subsets (m = myeloid; p = plasmacytoid; DC = dendritic cells) in protection against SIV acquisition for the four time points after boost investigated by transcriptomic analysis. The normalized enrichment score estimated by GSEA is plotted for each subset and separated by vaccine regimen (Ad26 – SIV, n = 11 animals; DNA – SIV, n = 12 animals). A normalized enrichment score (NES) > 0 or NES < 0 corresponds to markers of immune subsets enriched among genes associated with protection or SIV acquisition, respectively. GSEA two-tailed permutation test (fdr) was used to assess significance (sig) of the enrichments. (**b**) Boxplot showing that monocytes markers associated with protection identified in this study are expressed more in sorted classical monocytes than non-classical monocytes (subsets originated from n = 3 subjects). For each box on the plot, the median is indicated by a horizontal line, the box indicates the 1^{st} and 3^{rd} quartile of the values while the whiskers indicate the 1.5 interquartile range of the values. A two-tailed Student t-test was used to assess significance of the difference of expression between subsets. (**c**) NLP3 mRNA levels measured on PBMCs and sorted $CD14^-$ or $CD14^+$ cells in one non-vaccinated naïve macaque and one macaque in the DNA group (week 13) by RT-PCR.

Supplementary Figure 4. $CD16^+$ monocytes and STAT-3 activation correlate with increased SIV_{mac251} acquisition. (**a**) Frequency of monocytes expressing the CD16 marker (n = 12) correlates with risk of SIV acquisition (Spearman correlation, two-tailed, 95% confidence). (**b**) Line plot showing the normalized average expression of monocyte genes associated to SIV acquisition in each macaque (y-axis) as a function of the four time points after boosting with ALVAC-SIV+ gp120 (x-axis). (**c**) Scatter plot showing the normalized average expression of monocyte genes associated to acquisition in each macaque at week 25 (y-axis) as a function of the fraction of non-classical monocytes ($CD14^-$ $CD16^+$) among monocytes at week 27 (n = 12 animals). Linear regression fit (blue line) and its 95% confidence

interval (grey region) are given on the plot. (**d**) Network of the monocytes genes associated with acquisition of SIV of the DNA – SIV animals (n = 12 animals). The GeneMania inference method was used to identify co-expression, co-localization and common membership to canonical pathways (i.e. edges) between the monocyte genes (i.e. nodes). Each node is colored by the Pearson correlation of the genes (24h after the 2nd boost) with the number of SIV challenges to infection. (**e – g**) Phagocytic activity in serum after the last immunization measured in THP-1 cells, or in autologous cells (Ad26 group n = 12; DNA group n = 11).

Supplementary Figure 5. Differences in specific T cell responses induced by the two strategies at week 27 in blood. All vaccinated animals in the Ad26 group (n = 10) are in green circles, and those from the DNA (n = 9) are blue triangles. (**a**) IFN-γ, (**b**) IL-2, and (**c**) TNF-α producing CD4$^+$ T cells after *gag* stimulation in blood at 2 weeks after the last immunization (week 27). (**d**) IFN-γ, (**e**) IL-2, and (**f**) TNF-α producing CD8$^+$ T cells after *gag* stimulation in blood at 2 weeks after the last immunization (week 27). (**g**) IFN-γ, (**h**) IL-2, and (**i**) TNF-α producing CD4$^+$ T cells after *env* stimulation in blood at 2 weeks after the last immunization (week 27). (**j**) IFN-γ or (**k**) IL-2 and **(l**) TNF-α producing CD8$^+$ T cells after *env* stimulation in blood at 2 weeks after the last immunization (week 27). Each symbol represents one animal and the lines represent the medians (Ad26 group n = 10; DNA group n = 9). The Mann-Whitney-Wilcoxon nonparametric, two-tailed test was used to compare continuous factors between two groups.

Supplementary Figure 6. T cell responses induced by the two strategies at week 25 in bronchoalveolar lavage (BAL). (**a – e**) Responses in CD4$^+$ T cells, defined as CD3$^+$ and CD8$^–$, and in (**f – j**) CD8$^+$ T cells (CD3$^+$ CD8$^+$ cells). Each symbol represents one animal and the lines represent the medians. The Mann-Whitney-Wilcoxon nonparametric, two-tailed test was used to compare continuous factors between two groups (Ad26 group n = 12; DNA group n = 12).

Supplementary Figure 7. GATA3, key regulator factor of Th2 is increased in the DNA group after the prime. (**a**) PBMCs from 4 animals per group, collected at week 10 were stained for CD4$^+$ T cell detection and T-bet, GATA3, Rorγt intracellular expression. Plots for all the animals are shown gated within total CD4$^+$ T cells. Boxplots representing the min to max of cells positive for T-bet, Gata3 or Rorγt within CD4$^+$ T Ki67$^+$ T cells at 10 weeks (prime) or at week 13 (prime + boost), in 4 animals per group. The Mann-Whitney-Wilcoxon nonparametric, two-tailed test was used.

Supplementary Figure 8. Gating strategies for CD4$^+$ T cells and mucosal NKs. (**a**) Representative flow plot showing the gating strategy for measuring subsets of CD4$^+$ T helper cells or circulating T follicular helper cells (Tfh) in blood. Cells were gated on live and on Ki67$^+$ and CD95$^+$ cells or on CXCR5$^+$ Ki67$^+$ cells. CXCR3 and CCR6 were used to discriminate between Th1 (CXCR3$^+$ CCR6$^–$), Th2 (CXCR3$^–$ CCR6$^–$), and Th17 (CXCR3$^–$ CCR6$^+$) cells. (**b**) NKp44$^+$ cell measurement and mucosal recruitment. (**c**) Representative flow plot showing the gating strategy for measuring NKp44$^+$ or NKG2A$^+$ cells in the rectal mucosa. Mucosal NK cells were gated on live lymphocytes, which were negative for CD20 and CD3 and further classified based on the expression of NKG2A and NKp44 surface markers. (**c**) Frequency of NKp44$^+$ cells recruited at the mucosal site after ALVAC-primed (n = 27), Ad26-primed (n = 12), or DNA-primed (n = 11) ALVAC-SIV + gp120 alum vaccine and physiological levels in non-vaccinated controls (cntr). The Kruskal-Wallis test (nonparametric ANOVA) corrected for multiple comparisons was used.

Supplementary Figure 9. Differences in the antibodies responses induced by the two strategies at week 25 in plasma. All vaccinated animals in theAd26 group are in green circles, and those from the DNA are blue triangles. Mann-Whitney test was used. (**a**) IgG and (**b**) IgA titers in serum against the gp130 of SIV_{mac251} and (**c**) the gp140 of SIV_{smE660}. (**d**) Serum IgG titers to the gp70-V1/V2 scaffold of SIV_{mac251}. (**e**) Neutralizing antibodies to Tier1 $SIV_{mac251.6}$. (**f**) Specific activity of rectal IgG binding antibodies to the gp130 of SIV_{mac251} (**g**) and the gp140 SIV_{smE660}. (**h**) Specific activity of IgA and (**i**) IgG binding antibodies to the gp70-V1/V2 scaffold of $SIV_{mac251.6}$. (**j**) Mucosal IgG and (**k**) IgA responses to cyclic V2 measured as specific activity at week 25. Each symbol represents one animal and the lines represent the medians. The Mann-Whitney-Wilcoxon nonparametric, two-tailed test was used to compare continuous factors between two groups (Ad26 group n = 12; DNA group n = 12).

Supplementary Table 1: Cytokine production in rectal mucosa of the Ad26 and DNA prime groups at one week following the first (week 13) and last (week 25) ALVAC-SIV/gp120 alum. Cytokine production (ng/ml) from rectal mucosa cells collected with or without Env stimulation at week 13 (n = 7 Ad26; n = 7 DNA) and week 25 (n = 9 Ad26; n = 12 DNA). The Wilcoxon nonparametric, two-tailed test was used.

Supplementary Table 2. Genes associated with protection from SIV_{mac251} acquisition. (**a**) List of genes expressed differently between Ad26 (n = 12 animals) and DNA (n= 12 animals) primed animals using LIMMA two-tailed moderated t-test adjusted for multiple comparisons using the Benjamini-Hochberg correction. (**b**) List of genes correlated to the number of SIV challenge to acquisition using LIMMA two-tailed moderated t-test adjusted for multiple comparisons using the Benjamini-Hochberg correction. (**c**) List of pathways associated with SIV challenge to infection using GSEA two-tailed permutation test. (**d**) Monocyte genes associated with SIV challenge to infection.

Supplementary Table 3. Immune markers associated with the risk of SIV_{mac251} acquisition. (**a**) Full list of immune markers investigated (Dataset: type of experiment, Maker: immune marker measured). (**b**) List of markers significantly different between Ad26 (n = 11 animals) and DNA (n = 12 animals) groups using a Wilcoxon non-parametric, two-tailed test (p) adjusted for multiple comparisons using the Benjamini-Hochberg correction (adj.p). Difference of location column indicates the difference between the median expression in the Ad26 and DNA group. (**c**) Immune markers associated with SIV challenge to infection in a univariate analysis Spearman correlation (rho) and two-tailed Student *t*-test (p) adjusted for multiple comparisons using the Benjamini-Hochberg correction (adj.p). (**d**) Multivariate model associated with SIV challenge to infection using a two-tailed ANOVA *F*-test. The column reg. coef indicates the regression coefficient of the markers in the multivariate expression model.

Supplementary Table 4: Differentially expressed genes in the Ad26 and DNA primed animals. Differentially expressed genes in the Ad26 (n=11 animals) and DNA (n=12 animals) primed animals part of the NLRP3, HIF1a and IL10-STAT3 pathways. LIMMA two-tailed moderated t-test was used to assess significance of the differential expression.

Supplementary Table 5: SIV-specific adaptive B and T cell responses in the Ad26 prime and DNA prime groups at the end of the immunization regimen (week 27). Representations of these data can be found in Supplementary Figure 9.

Supplementary Table 6. Table summarizing cytokine and chemokine plasma levels following Ad26 and ALVAC prime at 24h, adapted from Ref. 41, 42.

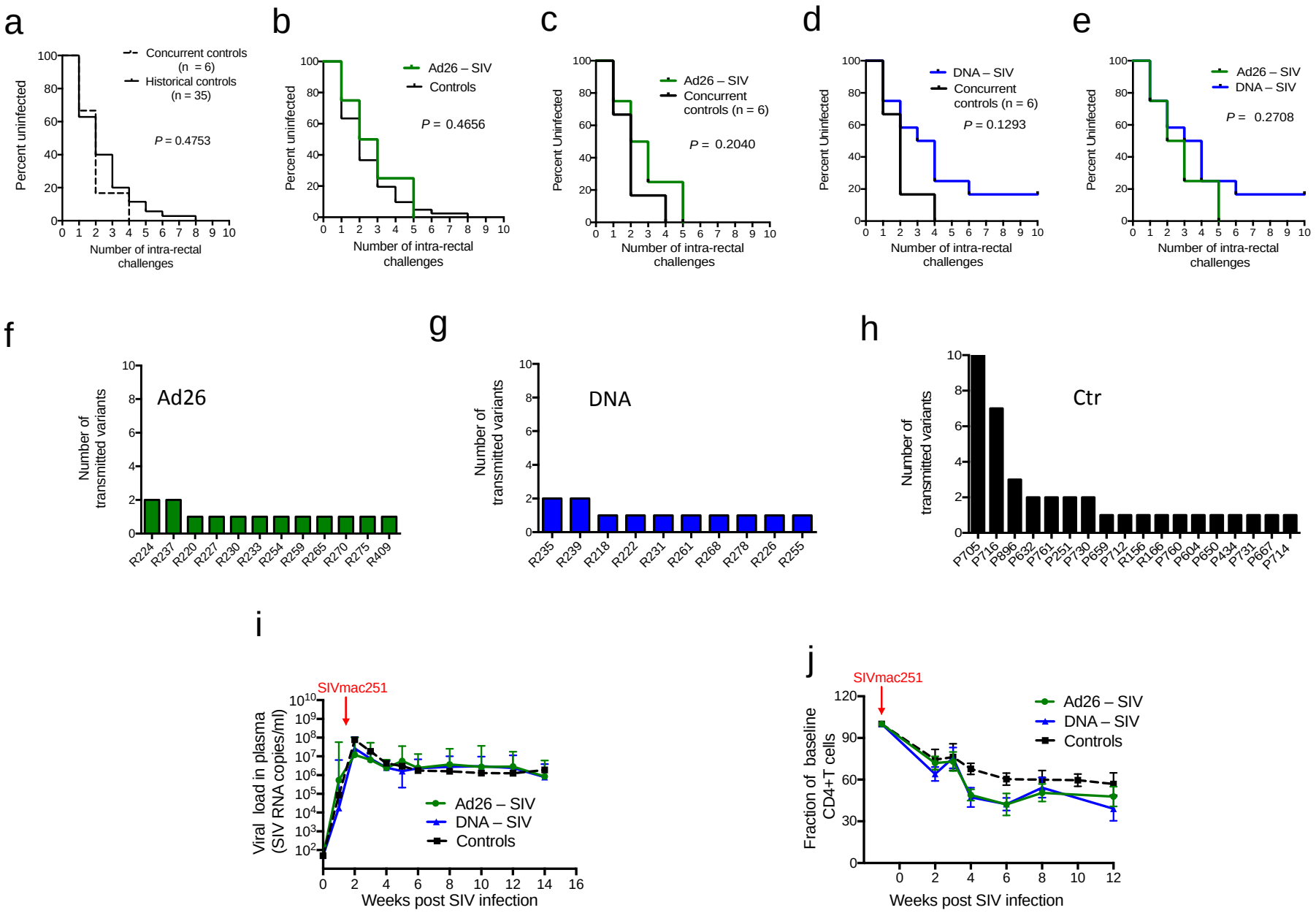

Supplementary Figure 1

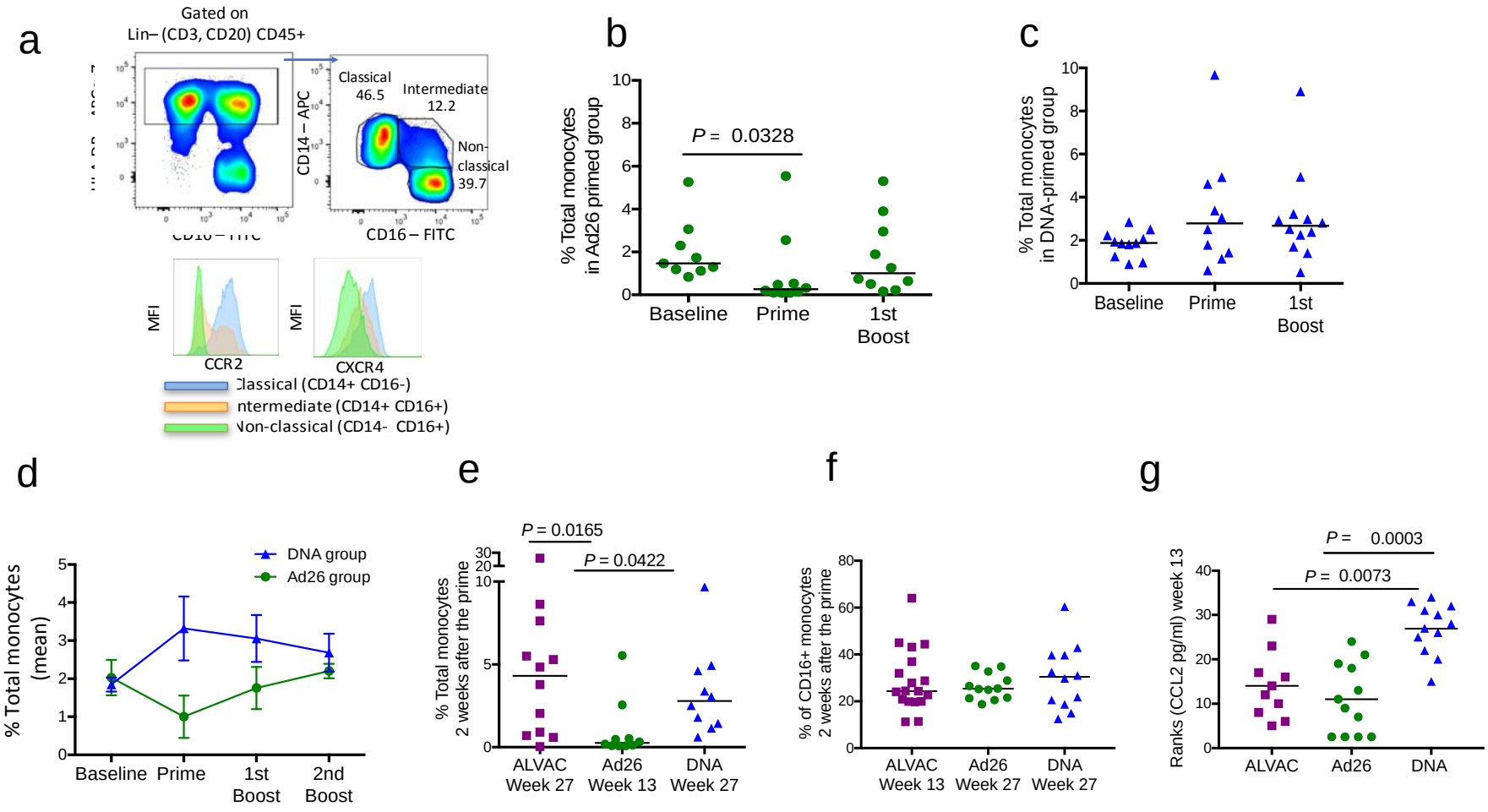

Supplementary Figure 2

a

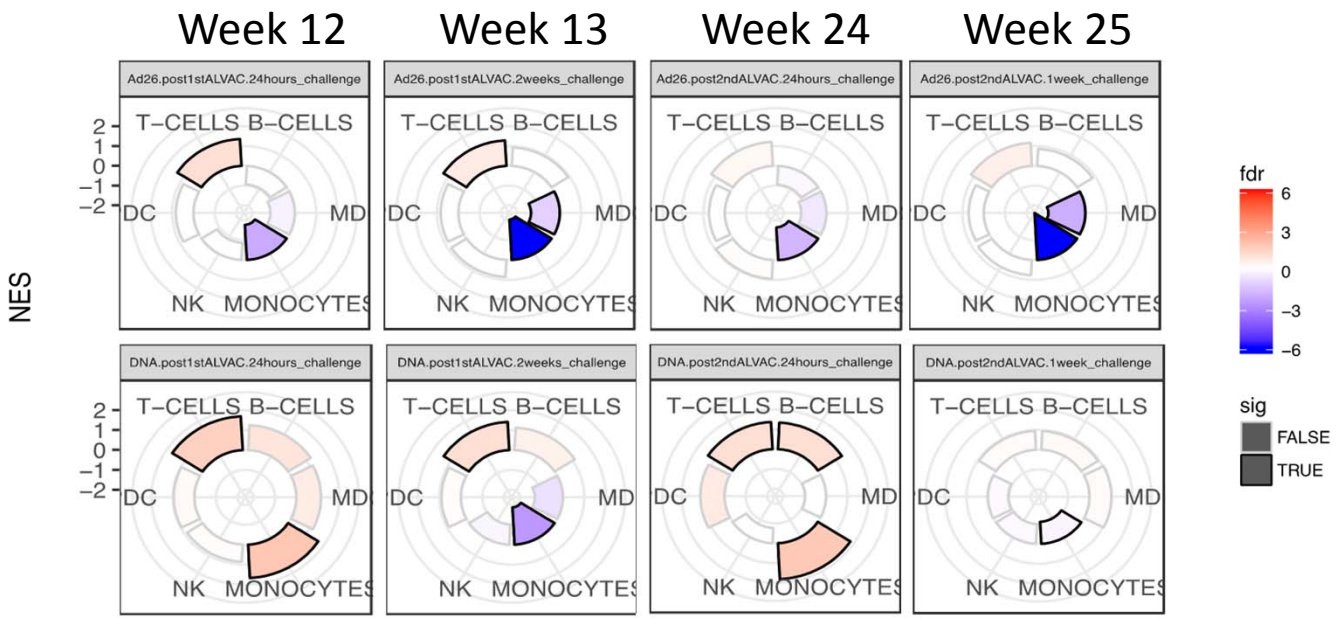

b

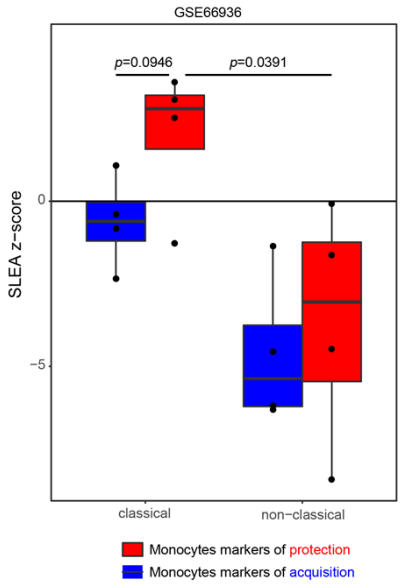

c

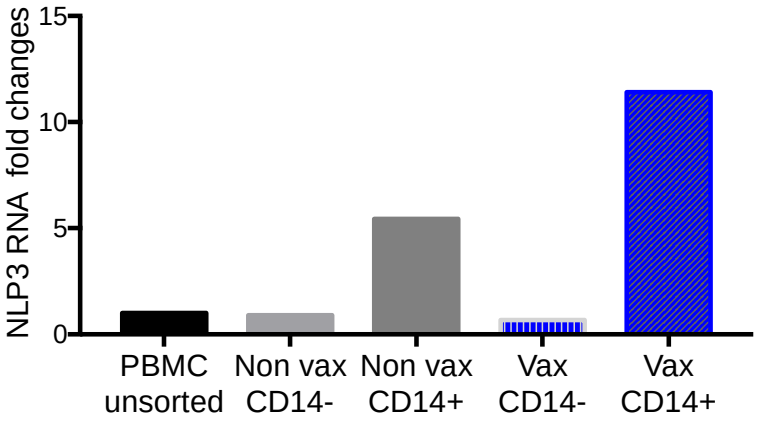

Supplementary Figure 3

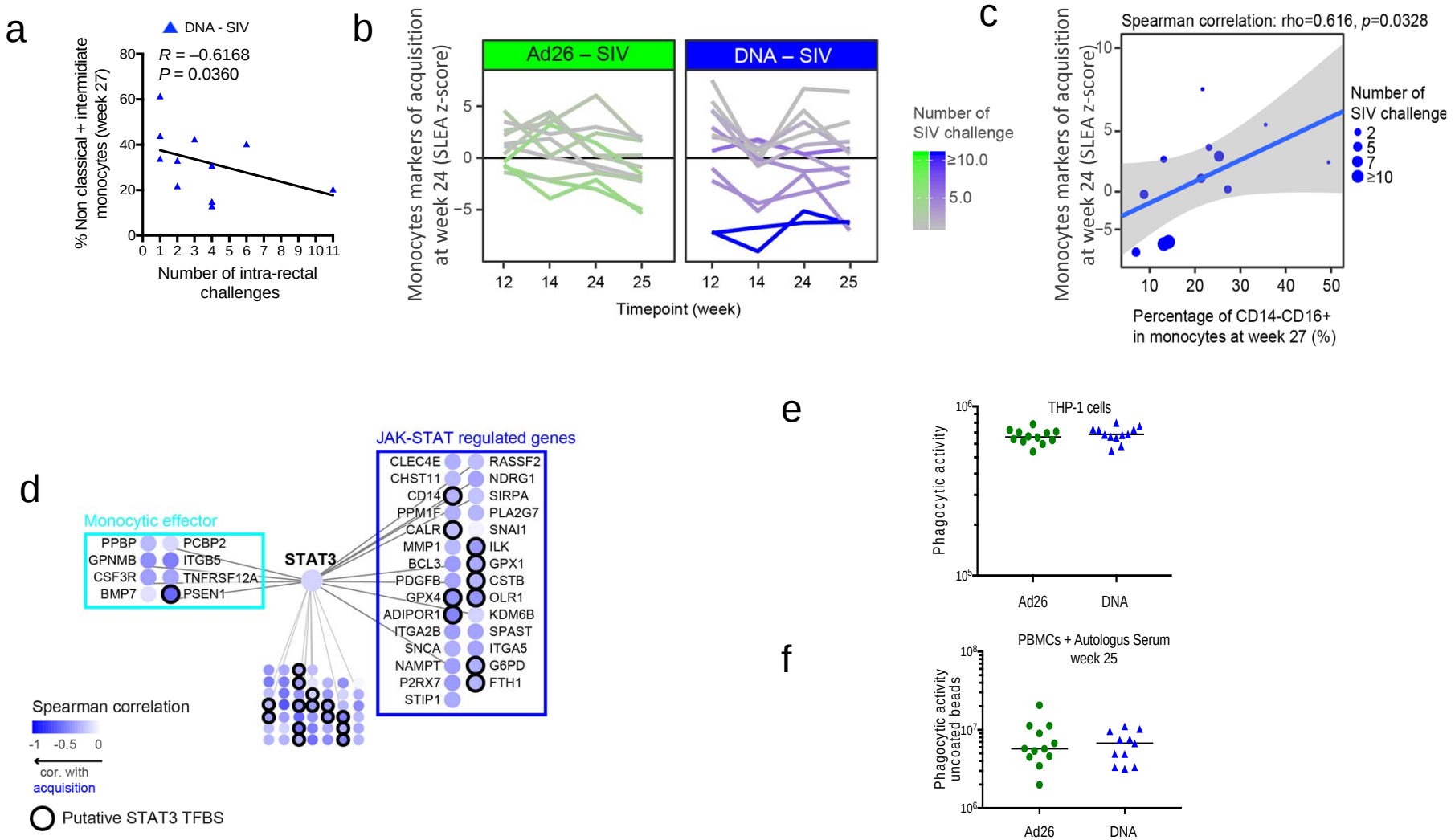

Supplementary Figure 4

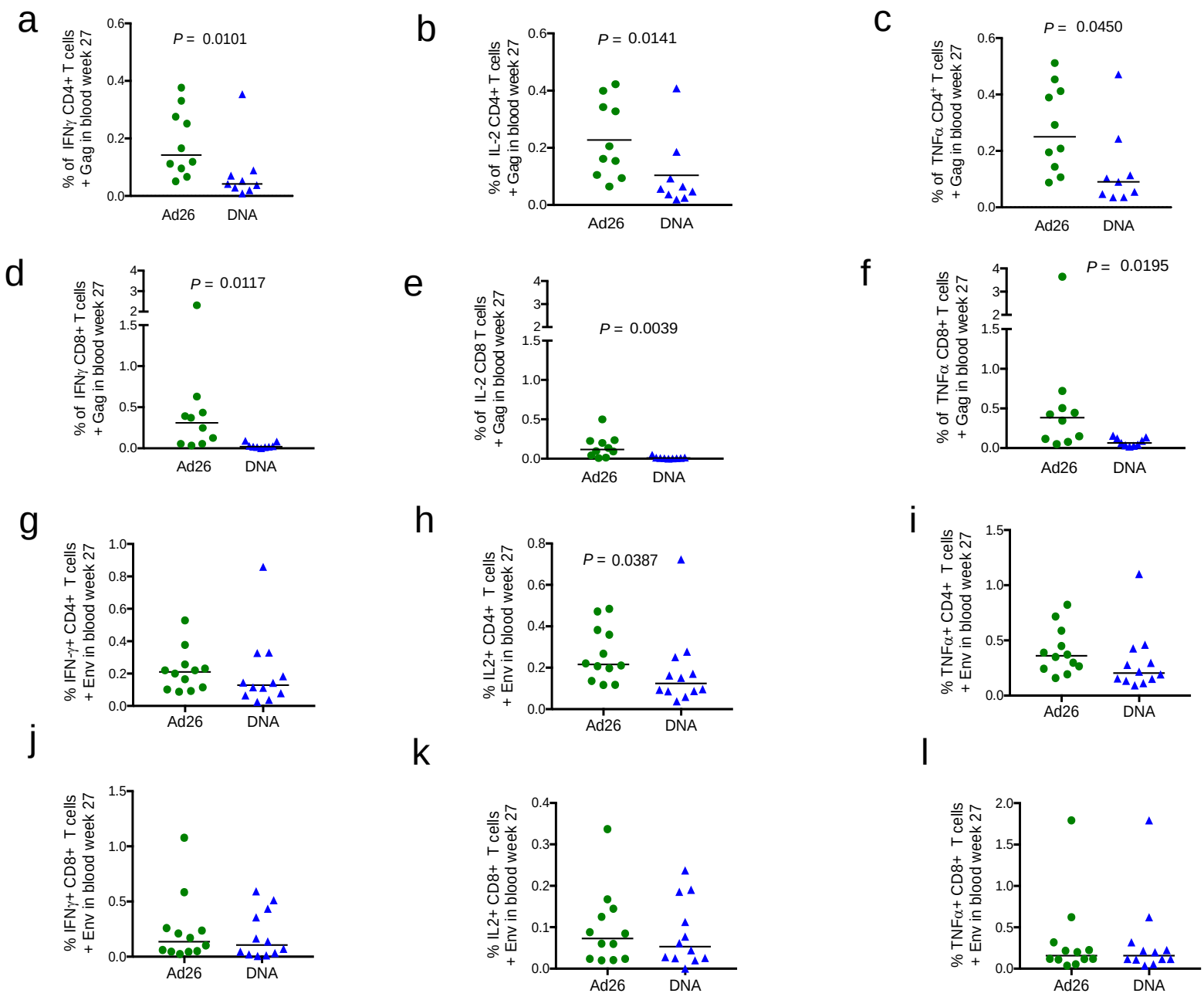

Supplementary Figure 5

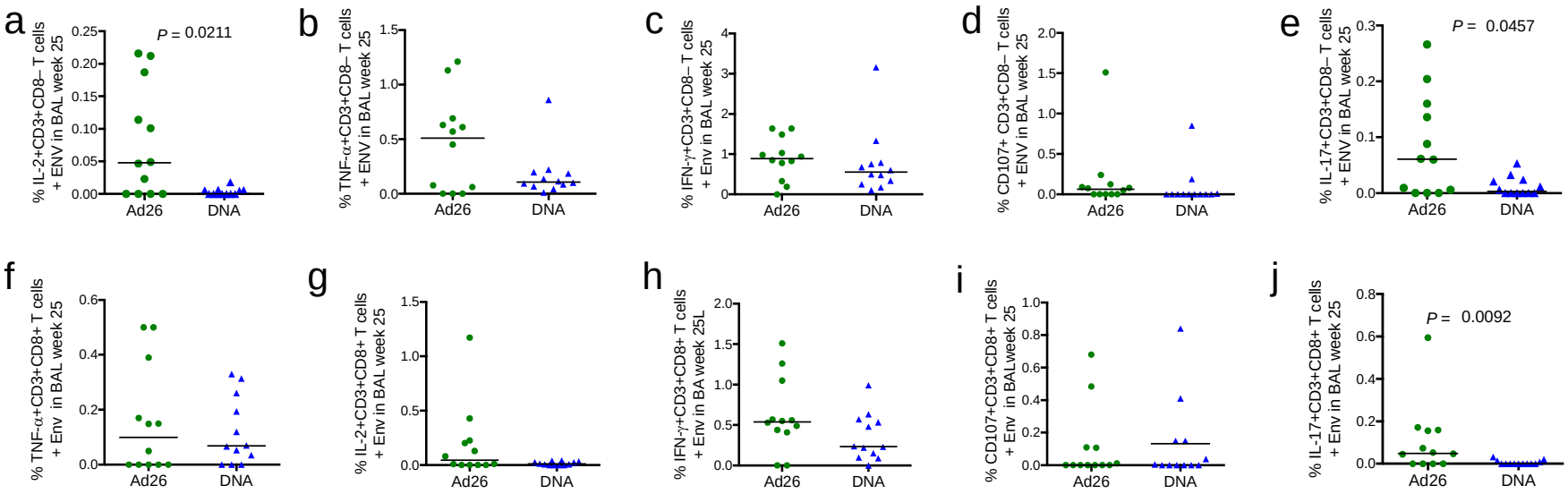

Supplementary Figure 6

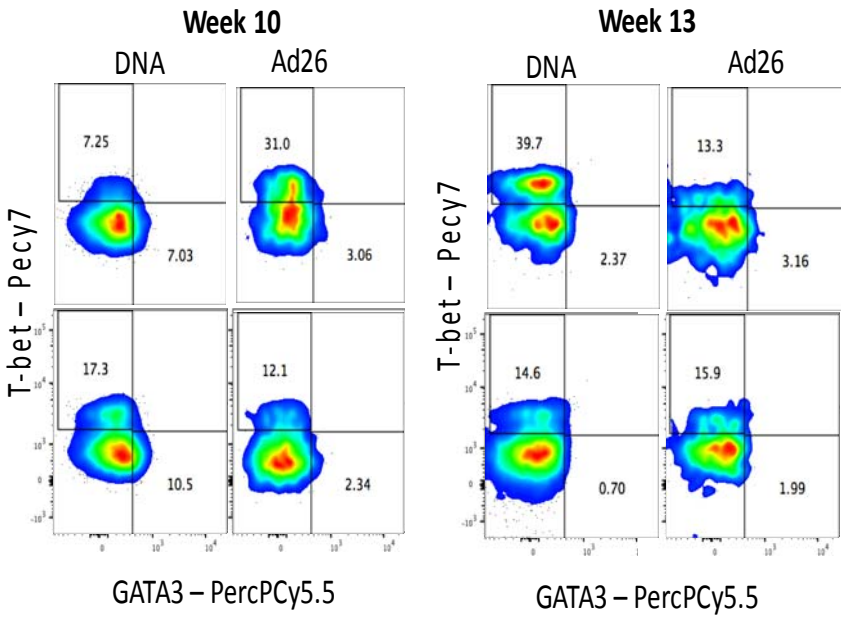

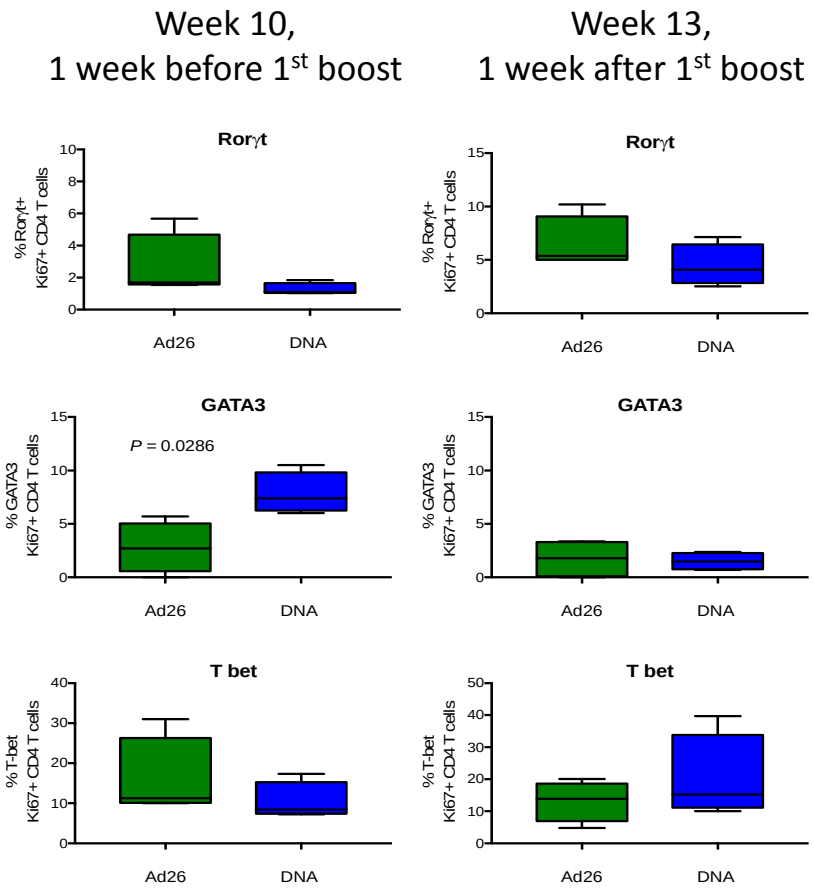

Supplementary Figure 7

a

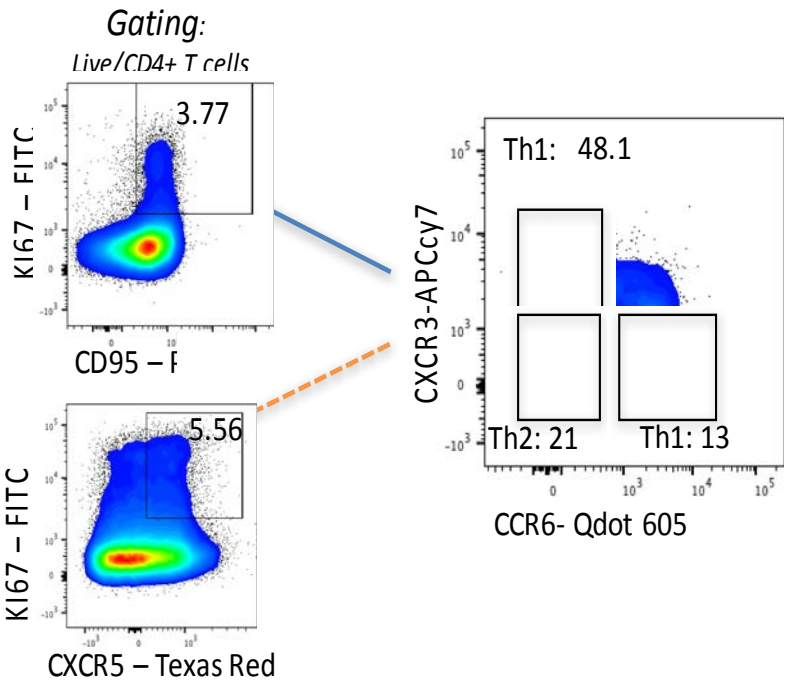

b

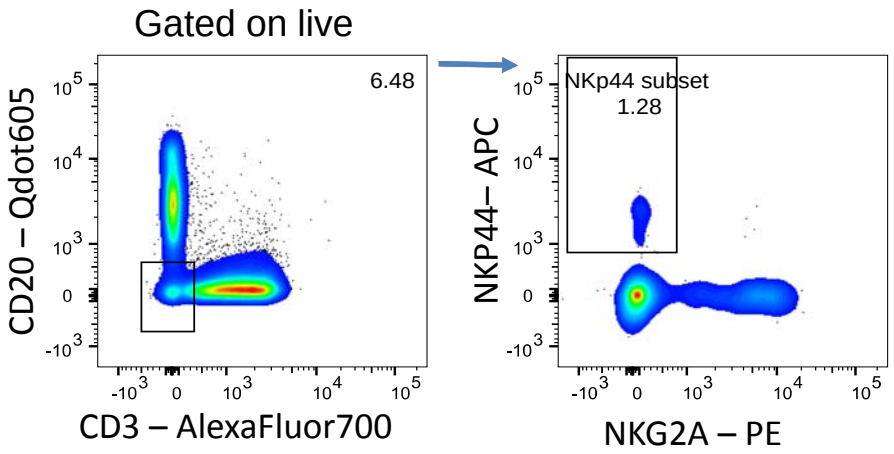

c

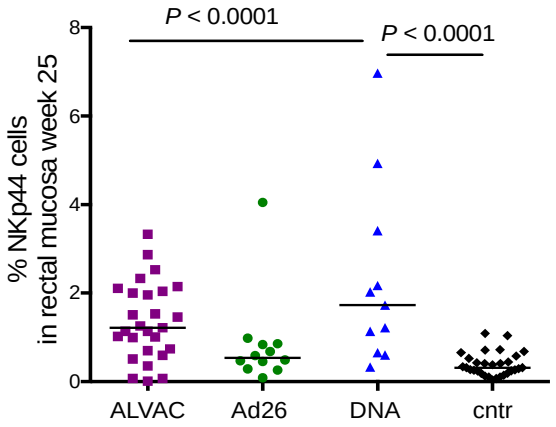

Supplementary Figure 8

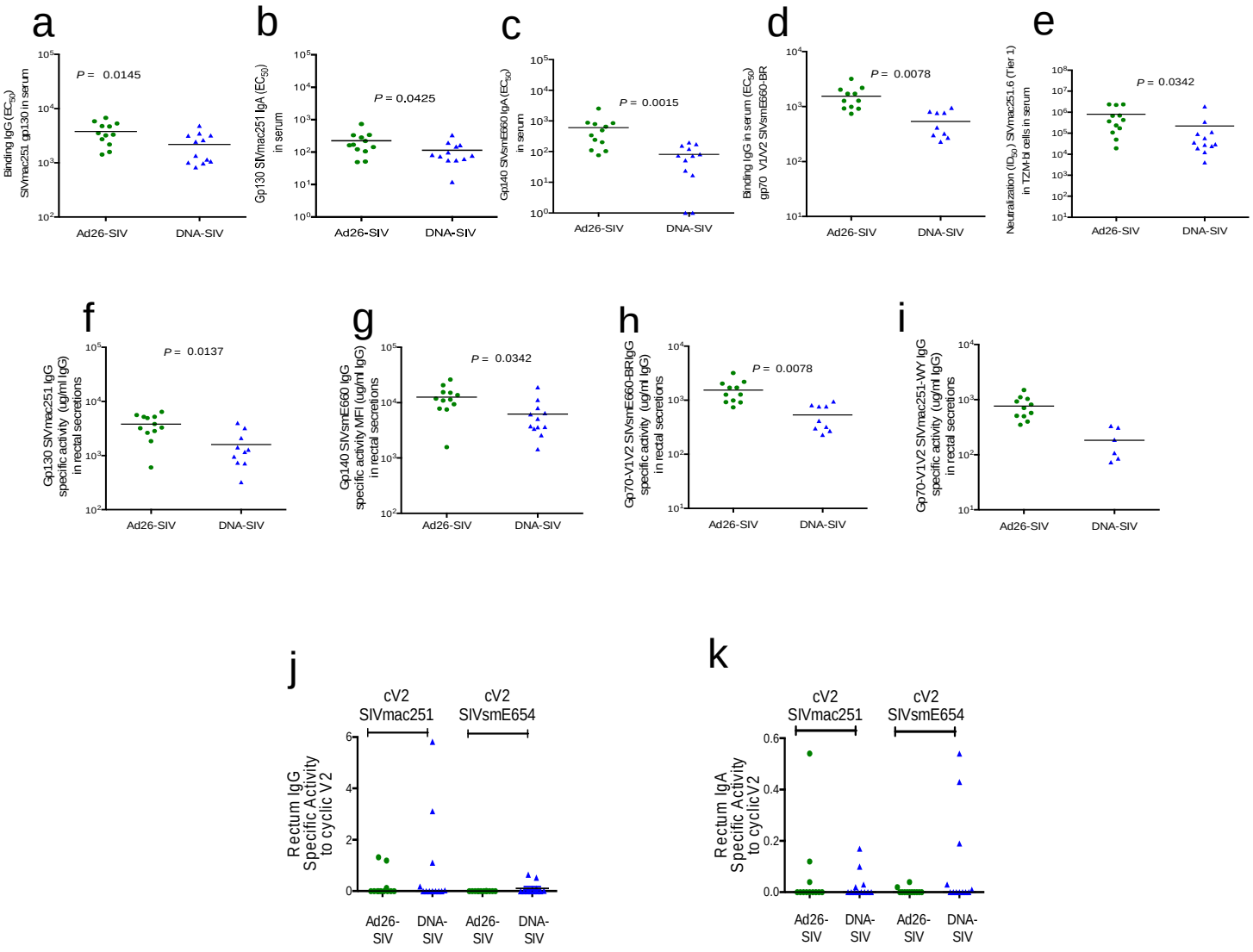

Supplementary Figure 9

	Wk 13 unstim			Wk 13 Env			Wk 25 unstim			Wk 25 Env		
	Ad26 median	DNA median	Mann Whitney P =	Ad26 median	DNA median	Mann Whitney P =	Ad26 median	DNA median	Mann Whitney P =	Ad26 median	DNA median	Mann Whitney P =
IL-1b	21.5	6.25	0.0012	19	8	0.0484	60	78	0.9852	55	56.5	0.9028
IL-2	17	2.5	0.0064	17	3.5	0.0472	17	16	0.5622	14	10	0.1739
IL-4	10.5	6.5	0.0676	14.5	6.5	0.2593	11	15	0.9555	9	9.5	0.9878
IL-6	258	49.5	0.0379	401	91.5	0.1527	359.5	587	0.5383	382.5	365.5	0.8078
IL-8	7752	1448.5	0.0041	8306	1536.5	0.0175	4107	3862	0.4119	4856	3229.25	0.0585
IL-10	32.8	3.8	0.007	34.8	11.8	0.0152	15	28	0.3598	25.5	25	0.917
IL-13	10.5	3.5	0.0047	20.5	4.5	0.1294	16.5	15.5	0.6682	17	17.5	0.4963
IL-17a	41.8	20.3	0.2086	34.8	22.3	0.1544	34	21	0.3215	31	36.5	0.7939
CCL2	6996.3	444.3	0.0023	6089.3	596.3	0.0041	5211	5967.5	0.5027	5258	4383	0.2773
CCL3	37	24	0.0262	27	19	0.1206	57.5	56	0.8396	46.5	40	0.716
IFN-g	27.5	3	0.0177	21.5	6.5	0.0657	25	14	0.0587	21.5	19.5	0.4963
CCL5	20	13	0.1055	19	13	0.4292	20	19	0.5511	18	28	0.0829
IL-23	4.5	3.5	0.9213	37.5	3.5	0.014	1.5	1.25	0.76	14	6	0.1502
IL-22	0.75	-5.3	0.0928	7.3	2.3	0.0954	-0.25	5.55	0.396	-0.3	0	0.5627
IL-21	7	3.5	0.0873	5.5	3.5	0.4211	4	5.25	0.7634	3.5	5.5	0.6946
TGF-b	2336	2393.5	0.9623	2591.5	2173.5	0.0002	2848.5	2635.5	0.1754	2689	2728.5	0.6556
TGF-b2	1149.25	1118.5	0.7396	1216.25	1123	0.0431	1188.5	1215.5	0.9575	1207	1202	0.882
TGF-b3	7.55	6.3	0.0341	8.3	4.8	0.004	8.3	7.8	0.1682	8.8	7.8	0.5606

Supplementary Table 1

	Immunization			Challenge			
	Model Name	t	p	Model Name	t	p	Function
NLRP3 inflammasome							
NLRP3	DNA.post1stALVAC.24hours-DNA.prevax	5.05	1.79E-06	DNA.post1stALVAC.24hours	1.71	0.107	
NLRP3				DNA.post1stALVAC.2weeks	1.46	0.163	
NLRP3	DNA.post2ndALVAC.24hours-DNA.prevax	6.61	1.46E-09	DNA.post2ndALVAC.24hours	3.22	0.00609	
HSP90AB1				DNA.post1stALVAC.24hours	1.28	0.218	
HSP90AB1				DNA.post2ndALVAC.24hours	1.27	0.224	
CASP1	DNA.post2ndALVAC.24hours-DNA.prevax.pre	11.9	2.13E-21	DNA.post2ndALVAC.24hours	2.60	0.0210	
IL1B				DNA.post1stALVAC.24hours	2.32	0.0345	
HIF1 signaling							
HIF1A	DNA.post1stALVAC.24hours-DNA.prevax.pre	3.14	0.00220	DNA.post1stALVAC.24hours	3.33	0.00443	
HIF1A	DNA.post2ndALVAC.24hours-DNA.prevax.pre	5.99	2.84E-08	DNA.post2ndALVAC.24hours	3.20	0.00637	
HIF1A	DNA.post2ndALVAC.1week-DNA.prevax.pre	1.99	0.0489	DNA.post2ndALVAC.1week	2.07	0.0566	
HIF1AN				DNA.post1stALVAC.2weeks	-1.58	0.133	HIF1 inhibitor
PPP1R12A				DNA.post1stALVAC.24hours	3.68	0.00213	HIF1 activator
PPP1R12A				DNA.post1stALVAC.2weeks	1.21	0.245	HIF1 activator
PPP1R12A	DNA.post2ndALVAC.24hours-DNA.prevax.pre	4.53	1.52E-05	DNA.post2ndALVAC.24hours	3.41	0.00422	HIF1 activator
ARNT2				DNA.post1stALVAC.2weeks	1.36	0.192	cofactor of HIF1A
IL10-STAT3							
STAT3				DNA.post1stALVAC.24hours	-1.63	0.124	
STAT3				DNA.post1stALVAC.2weeks	-3.59	0.00239	
TNFRSF1A				DNA.post1stALVAC.24hours	-1.43	0.174	IL10 positively regulates extracellular inflammatory mediators
TNFRSF1A				DNA.post1stALVAC.2weeks	-4.31	0.000506	IL10 positively regulates extracellular inflammatory mediators
TNFRSF1A				DNA.post2ndALVAC.1week	-1.95	0.0715	IL10 positively regulates extracellular inflammatory mediators
TIMP1				DNA.post2ndALVAC.24hours	-1.31	0.212	IL10 positively regulates extracellular inflammatory mediators
Il1RN				DNA.post1stALVAC.2weeks	-1.35	0.197	IL10 positively regulates extracellular inflammatory mediators

Supplementary Table 4

B Cell Responses Week 27		Mann Whitney P Value		T Cell Responses Week 27		Mann Whitney P Value
	SERUM	Ad26 > DNA			BLOOD	Ad26 > DNA
	bAb IgG mac251 (EC50)	0.0145			Env m766 ICS CD4 IFN-g	ns
	bAb IgG E660 (EC50)	ns			Env m766 ICS CD4 TNF-a	ns
	bAb IgG V1V2 mac251 WY (EC50)	ns			Env m766 ICS CD4 IL-2	0.0387
	bAb IgG V1V2 E660 BR (EC50)	ns				
	bAb IgA 251 (MFI)	0.0861			Gag m766 ICS CD4 IFN-g	0.0101
	bAb IgA E660 (MFI)	0.0003			Gag m766 ICS CD4 TNF-a	0.0279
	Titers IgG mac251 cyclic V2	ns			Gag m766 ICS CD4 IL-2	0.0141
	Titers IgG E543 cyclic V2	ns				
	Titers IgA mac251 cyclic V2	ns (0.078)			Env m766 ICS CD8 IFN-g	ns
	Titers IgA E543 cyclic V2	ns (0.068)			Env 766 ICS CD8 TNF-a	ns
	RECTUM				Env m766 ICS CD8 IL2	ns
	nAb DM SIVmac251 Stock	ns			Gag m766 ICS CD8 IFN-g	0.0006
	nAb DM SIVmac251 Tier 1	0.0067			Gag m766 ICS CD8 TNF-a	0.0076
	Specific activity mac251 gp130	< 0.0001			Gag m766 ICS CD8 IL-2	0.001
	Specific activity E660 gp130.	< 0.001			BAL	
	Specific activity V1V2 mac251	< 0.001			Env IL-2 $CD8^-$	0.021
	Specific activity V1V2 E660	< 0.001			Env TNF-a $CD8^-$	ns
		Ad26 = DNA			Env IFN-g $CD8^-$	ns
	Specific activity IgG mac251 cyclic V2	ns (0.078)			Env CD107 $CD8^-$	ns
	Binding IgG E543 cyclic V2	ns (0.068)			Env IL-17 $CD8^-$	0.045
	Binding IgA E543 cyclic V2	ns (0.504)			Env IL-2 $CD8^+$	ns
	Binding IgA mac251 cyclic V2	ns (0.417)			Env TNF-a $CD8^+$	ns
					Env IFN-g $CD8^+$	ns
					Env CD107 $CD8^+$	ns
					Env IL-17 $CD8^+$	0.0092

Supplementary Table 5

	ALVACgpe	Ad26gpe	MVAgpe
IFNalpha	< 1.5	nd	< 1.5
IL-2	1.5 – 2	< 1.5	< 1.5
TNF-alpha	**10 – 50**	< 1.5	< 1.5
IFN-gamma	< 1.5	1.5 – 2	< 1.5
IP10	1.5 – 2	**5 – 10**	2 – 5
IL-5	1.5 – 2	< 1.5	< 1.5
IL-6	**> 50**	2 – 5	1.5 – 2
TGF-alpha	2 – 5	< 1.5	< 1.5
IL-10	**10 – 50**	nd	< 1.5
IL-17	< 1.5	< 1.5	< 1.5
IL-12/23	< 1.5	< 1.5	< 1.5
IL-8	< 1.5	< 1.5	< 1.5
IL-1b	**> 50**	< 1.5	< 1.5
IL-1Ra	**10 – 50**	**5 – 10**	< 1.5
MIP-1beta	**5 – 10**	< 1.5	< 1.5
CCL2	2 – 5	< 1.5	< 1.5
VEGF	**5 – 10**	< 1.5	< 1.5

Supplementary Table 6